Am J Transl Res 2025;17(8):6320-6332
www.ajtr.org /ISSN:1943-8141/AJTR0166114

Original Article

Tricuspid annular dilation and occluder deviation predict worsening of tricuspid regurgitation after transcatheter closure of atrial septal defect with patent foramen ovale

Xuejia Guo, Na Wang, Ya Liu, Miaomiao Pei, Gaiqin Liu, Yanyan Zhang, Ning Zhang

Department of Ultrasound, The First Hospital of Hebei Medical University, Shijiazhuang 050000, Hebei, China

Received May 17, 2025; Accepted July 27, 2025; Epub August 15, 2025; Published August 30, 2025

Abstract: Objective: To evaluate the predictive value of echocardiographic findings for postoperative tricuspid regurgitation (TR) worsening after transcatheter atrial septal defect (ASD) with patent foramen ovale (PFO) closure using domestic occluders, and to develop a dynamic risk prediction model to guide clinical decision-making. Methods: This retrospective cohort study included 109 patients undergoing ASD/PFO closure with occluders (manufactured domestically in China) at a single center (between January 2018 and May 2024). Participants were stratified into an observation group (TR worsening ≥ 1 grade, n = 26) and a control group (stable TR, n = 83). Echocardiographic data - including tricuspid annular diameter, coaptation height, and occluder positional deviation - were assessed preoperatively, immediately postoperatively, and at 1-year follow-up. Univariate and multivariate logistic regression analyses were performed to identify independent predictors. Model performance was evaluated using receiver operating characteristic (ROC) curves. Results: Compared to controls, the observation group (n = 26) exhibited significantly greater tricuspid annular dilation (mean Δdiameter: 3.2 ± 0.8 mm vs 0.9 ± 0.4 mm; P < 0.001) and occluder positional deviation (4.1 ± 1.2 mm vs 1.8 ± 0.6 mm; P < 0.001). Multivariate analysis identified Δtricuspid annular diameter (OR = 1.32 per 1-mm increase, 95% CI: 1.12-1.56; P < 0.001) and occluder deviation (OR = 2.41 per 1-mm increase, 95% CI: 1.68-3.45; P < 0.001) as independent predictors of TR worsening. The combined predictive model demonstrated superior discrimination (AUC = 0.802, 95% CI: 0.742-0.862; sensitivity = 76.9%, specificity = 81.3%) outperforming their individual application (P < 0.001). Subgroup analysis showed consistent predictive performance across occluder types ($P_{interaction}$ = 0.87). Conclusion: Dynamic tricuspid annular dilation and occluder malposition erre independent risk factors for postoperative TR progression. The echocardiography-based predictive model enhances risk stratification and may inform intraprocedural adjustments and postoperative surveillance.

Keywords: Tricuspid regurgitation, atrial septal defect, patent foramen ovale, echocardiography, risk prediction

Introduction

Atrial septal defect (ASD) with concomitant patent foramen ovale (PFO) accounts for approximately 15-20% of adult congenital heart disease cases globally, with transcatheter closure emerging as the standard therapy due to its minimally invasive nature and high success rate [1]. In China, domestically manufactured occluders have gained widespread adoption, demonstrating comparable mid-term efficacy to international devices [2]. However, postoperative tricuspid regurgitation (TR) worsening remains a significant concern, affecting 12-18% of patients within one year of device implantation [3]. This complication correlates strongly with adverse clinical outcomes, including an increased risk of right heart failure and 5-year mortality [4].

Current risk stratification models for post-closure TR rely predominantly on baseline clinical factors (e.g., age, pulmonary hypertension) or static anatomic measurements (e.g., preprocedural annular diameter) [5], neglecting dynamic echocardiographic changes during and after intervention. Emerging evidence suggests that procedural factors, particularly device-related mechanical interactions with the tricuspid apparatus play a pivotal role in TR pathogenesis. 3D echocardiographic studies have revealed that malpositioned occluders induce asym-

https://doi.org/10.62347/MGNQ6995

metric annular distortion, increasing leaflet tethering forces [6]. Despite these insights, no validated predictive tools integrate intraprocedural echocardiographic metrics, such as real-time annular dynamics or positional deviation, to guide risk assessment [7]. This gap persists even with advancements in quantitative echocardiography, including speckle-tracking annular strain analysis and 4D flow imaging, which enable precise characterization of valvular biomechanics [8].

Recent investigations highlight the potential of longitudinal echocardiographic monitoring in predicting TR progression. An 18-year retrospective study demonstrated that preoperative TR in patients with ASD was independently associated with increased all-cause mortality [9]. Another study identified age ≥ 60 years, right atrial end-diastolic area ≥ 10 cm^2/m^2, right ventricular systolic pressure ≥ 44 mmHg, and tricuspid annular plane systolic excursion ≤ 2.3 cm as independent predictors of moderate-to-severe TR after transcatheter closure [10]. Despite these advancements, critical gaps persist in translating biomechanical insights into clinically actionable tools. Established predictors such as age and right ventricular pressure are static and fail to capture the dynamic interplay between device implantation and annular remodeling across the preoperative, intraoperative, and postoperative phases.

This study aimed to develop and validate an echocardiography-based predictive model for postoperative TR worsening following transcatheter ASD/PFO closure using domestically manufactured occluders. Innovatively, this research incorporates dynamic intraprocedural tricuspid annular dilation and occluder-device interaction metrics as key predictors, moving beyond traditional static preoperative measurements. It represents the first risk-stratification tool integrating real-time echocardiographic dynamics specifically for domestically manufactured devices. Clinically, this model enables (1) immediate procedural adjustments to optimize occluder positioning, (2) personalized post-operative surveillance for high-risk patients, and (3) improved long-term valve outcomes in resource-limited settings in which domestic occluders broaden treatment accessibility.

Methods

Patient selection, inclusion/exclusion criteria, and search methods

This retrospective cohort study enrolled patients who underwent transcatheter closure of ASD with PFO using domestic occluder devices at The First Hospital of Hebei Medical University between January 2018 and May 2024. The study protocol was approved by the Institutional Review Board of The First Hospital of Hebei Medical University (Approval No.: 20220680), and the requirement for informed consent was waived due to the retrospective nature of the analysis. Electronic medical records and echocardiographic databases were systematically reviewed to identify eligible patients based on predefined inclusion and exclusion criteria. Data collection included preoperative, intraoperative, and follow-up echocardiographic parameters, as well as clinical and procedural characteristics, to evaluate predictors of postoperative tricuspid regurgitation (TR) worsening. The study adhered to the principles of the Declaration of Helsinki and ensured patient confidentiality through anonymized data handling.

Electronic medical records and dedicated cardiac imaging databases were systematically queried using International Classification of Diseases (ICD-10) codes for ASD (Q21.1) and PFO (Q21.1) and procedural codes for transcatheter closure (35.52, 35.55, 35.62). Initial screening identified 118 potential candidates.

Patients diagnosed with ASD concomitant with PFO who underwent transcatheter closure using domestically manufactured occluder devices were eligible for inclusion. Inclusion criteria: (1) availability of complete echocardiographic data at baseline, immediately postoperative, and 1-year follow-up; (2) age ≥ 18 years; and (3) absence of prior cardiac surgical interventions. Exclusion criteria: (1) history of valvular surgery or significant structural valvular abnormalities (e.g., congenital tricuspid valve dysplasia); (2) severe pulmonary hypertension (defined as resting systolic pulmonary artery pressure ≥ 50 mmHg confirmed by echocardiography or right heart catheterization); (3) coexisting complex congenital heart defects (e.g., tetralogy of Fallot); and (4) incomplete clinical or imaging records (**Figure 1**).

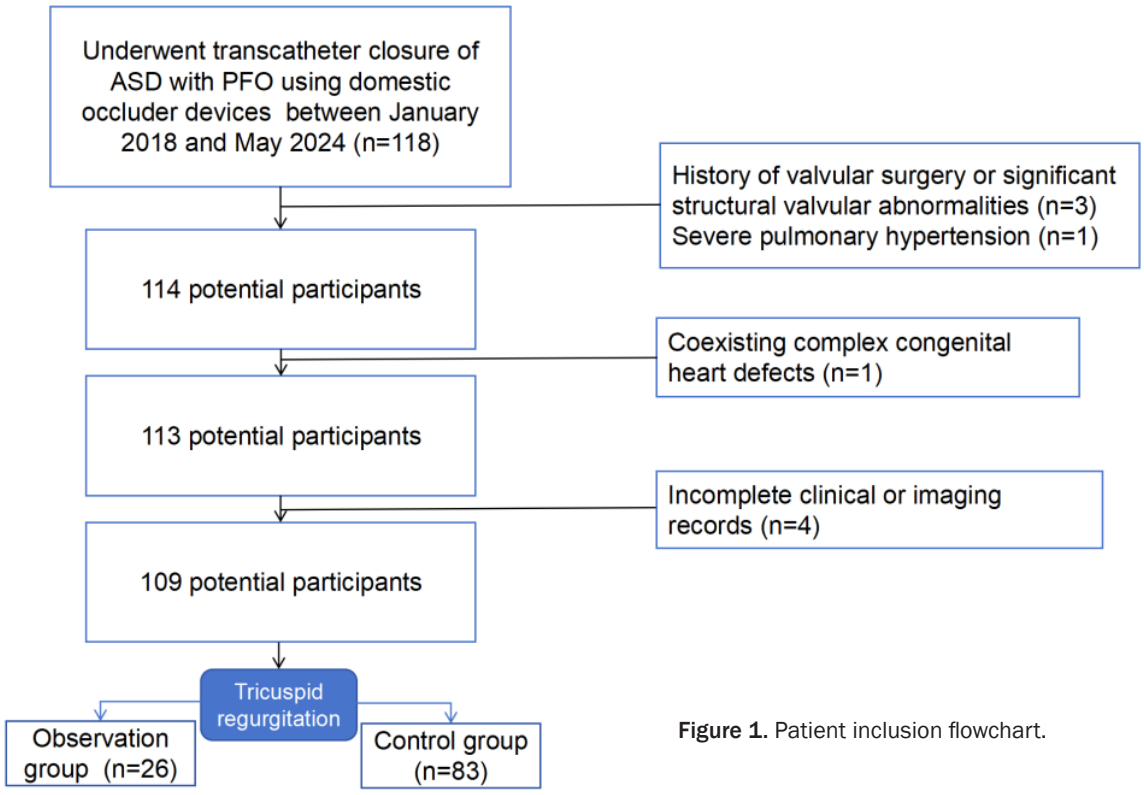

Figure 1. Patient inclusion flowchart.

Participants were stratified into two groups based on postoperative tricuspid regurgitation (TR) progression at 1-year follow-up: the observation group (TR worsening ≥ 1 grade according to the American Society of Echocardiography (ASE) guidelines [11]) and the control group (no TR worsening or stable TR grade). TR severity was assessed by comprehensive echocardiographic evaluation, including vena contracta width, regurgitant jet area, and quantitative Doppler measurements.

Data extraction methods, variables, and validation

Echocardiographic, procedural, and clinical data were systematically extracted from institutional electronic health records (Cerner Millennium®) and cardiac PACS archives (Philips IntelliSpace®) by three independent cardiologists blinded to patient outcomes. Standardized quantification protocols per American Society of Echocardiography guidelines [11] were applied to evaluate: 1) tricuspid valve morphology (annular diameter in the apical 4-chamber view, tricuspid annular plane systolic excursion (TAPSE), and coaptation height); 2) hemodynamic measurements (right ventricular systolic pressure (RVSP) calculated by modified Bernoulli equation $\Delta P = 4v^2$, right atrial (RA)/right ventricular (RV) volumes indexed to body surface area (BSA)); 3) device-related metrics (occluder positional deviation assessed by fluoroscopic-echocardiographic co-registration, device morphology, size); and 4) clinical variables (demographics, procedural duration, occluder model).

Validation included inter-rater reliability assessment (intraclass correlation coefficient (ICC) > 0.85 for continuous variables), consensus adjudication for categorical discrepancies, periodic auditing of 10% random selected samples by a senior echocardiologist, and averaging of continuous Doppler measurements over three cardiac cycles. Data abstraction was performed using REDCap electronic case report forms with automated range checks to ensure integrity.

Outcome measurement

TR progression was evaluated as the primary clinical outcome, defined as ≥ 1-grade increase in TR severity from baseline to 1-year follow-up

using ASE multiparametric criteria [11]. These criteria incorporated vena contracta width increase ≥ 0.3 cm, jet area expansion ≥ 30%, and new systolic flow reversal in hepatic veins or effective regurgitant orifice area (EROA) ≥ 0.2 cm^2.

Secondary outcomes included device-related complications: Arrhythmias: new-onset atrial fibrillation (AF) or atrioventricular (AV) block confirmed by 12-lead ECG; Device embolization: based on radiographic/echocardiographic evidence; Pericardial effusion: ≥ 5 mm diastolic effusion on transthoracic echocardiography (TTE); Hemolysis: Hb drop ≥ 2 g/dL with lactate dehydrogenase (LDH) > 250 U/L and negative Coombs test; Vascular complications: access-site hematoma requiring intervention.

Additional endpoints included right heart remodeling measurements, such as changes in tricuspid annular diameter and right atrial volume index. All outcomes were evaluated at three standardized time points: preoperative (baseline), immediate postoperative (≤ 24 h), and 1-year follow-up (± 30 days).

Sample size calculation

Given the binary nature of the primary outcome of TR progression, we conducted an *a priori* sample size estimation for multivariable logistic regression using the standard formula: the required sample size equals the square of the sum of Z-values for type I and II errors, divided by the product of event probability times (1 minus event probability) times the squared log-odds ratio of the key predictor, then multiplied by the inverse of (1 minus R-squared). Specifically, we set a two-sided α of 0.05 (Z = 1.96) and β of 0.20 for 80% power (Z = 0.84), with an expected event probability of 32.6% from pilot data. Using an odds ratio of 2.5 for annular dilation (β = log (2.5)) derived from prior literature and estimating covariate correlation (R^2 = 0.3), the calculation yielded 152 subjects. Accounting for 15% potential data loss, the target enrollment was set at 175. The final cohort comprised 172 patients, providing > 90% power to detect odds ratios ≥ 2.0 for primary predictors while maintaining an events-per-variable ratio of 11.2 (56 events ÷ 5 predictors), exceeding the recommended threshold of 10 for model stability.

Statistical analysis

Univariate analyses identified potential predictors of TR worsening, employing appropriate statistical tests based on variable characteristics and distributional properties. Continuous variables such as annular diameter and RVSP were compared using independent Student's t-tests when normality assumptions were satisfied (verified by Shapiro-Wilk tests) or Mann-Whitney U tests for non-normally distributed data. Categorical variables including device type and sex were analyzed by chi-square or Fisher's exact tests as appropriate for cell frequencies. Variables demonstrating significant associations (P < 0.1) in univariate analysis were eligible for inclusion in the multivariate logistic regression model. This model was constructed using backward stepwise elimination with likelihood ratio criterion, removing variables exceeding a threshold of P > 0.1 at each step. Reference categories were specified as mild TR (baseline grade) for TR severity comparisons and symmetric occluder for device type evaluations, while continuous predictors were scaled per 1-mm increment (e.g., ΔAnnular Diameter, Positional Deviation). The final model provided adjusted odds ratios (ORs) with 95% confidence intervals (CIs), alongside regression coefficients (β), standard errors (SE), Wald χ^2 statistics, and degrees of freedom (df). Model discrimination was evaluated through receiver operating characteristic (ROC) curve analysis, with area under the curve (AUC), sensitivity, and specificity calculated. Optimal cutoffs were determined by Youden's index. Subgroup consistency was further assessed using Bland-Altman plots and formal interaction tests. Statistical significance for all analyses was defined as two-tailed P < 0.05. All analyses were performed using SPSS 26.0 and R version 4.2.1 (package pROC and BlandAltmanLeh).

Results

Baseline characteristics comparison

A total of 218 patients (observation group: n = 26; control group: n = 83) were included in the final analysis. The overall cohort had a mean age of 42.3 ± 12.7 years, with a female predominance (63.3%). Baseline demographic, clinical, and lifestyle characteristics were well-

Table 1. Baseline demographic, clinical, and lifestyle characteristics

Variable	Observation Group (n = 26)	Control Group (n = 83)	Statistical Value (t or χ^2)	*P*-value
Age (years)	43.1 ± 11.9	42.0 ± 13.0	0.547	0.590
Female, n (%)	17 (65.4%)	52 (62.7%)	0.134	0.720
BMI (kg/m^2)	24.3 ± 3.5	23.8 ± 3.2	0.912	0.364
Comorbidities				
Hypertension, n (%)	8 (30.8%)	23 (27.7%)	0.194	0.663
Diabetes Mellitus, n (%)	3 (11.5%)	11 (13.3%)	0.125	0.729
Atrial Fibrillation, n (%)	2 (7.7%)	6 (7.2%)	0.023	0.902
Lifestyle Factors				
Smoking History, n (%)	6 (23.1%)	17 (20.5%)	0.185	0.673
Alcohol Consumption, n (%)	5 (19.2%)	14 (16.9%)	0.011	0.940
Cardiac Parameters				
LVEF (%)	58.2 ± 5.1	57.8 ± 4.9	0.493	0.625
NYHA Class II/III, n (%)	9 (34.6%)	28 (33.7%)	0.044	0.841
Preoperative TR Grade				
Mild	20 (76.9%)	66 (79.5%)	0.182	0.670
Moderate	6 (23.1%)	17 (20.5%)		
RVSP (mmHg)	32.4 ± 6.2	31.8 ± 5.9	0.622	0.540
Right Atrial Volume (mL/m^2)	41.5 ± 8.7	40.2 ± 9.1	0.931	0.354
Procedural Data				
Occluder Type, n (%)				
Symmetric	17 (65.4%)	58 (69.9%)	0.080	0.780
Asymmetric	8 (30.8%)	26 (31.3%)		

Note: BMI, body mass index; LVEF, left ventricular ejection fraction; NYHA, New York Heart Association; TR, tricuspid regurgitation; RVSP, right ventricular systolic pressure. Statistical Tests: Independent t-test (parametric), Mann-Whitney U test (non-parametric), or χ^2/Fisher's exact test (categorical).

balanced between the two groups (**Table 1**). No significant differences were observed in age, sex distribution, body mass index (BMI), comorbidities (hypertension, diabetes mellitus), smoking/alcohol history, or preoperative cardiac data (all P > 0.05). Hypertension (28.4%) and diabetes (12.8%) were the most prevalent comorbidities, and 21.1% of patients reported a history of smoking. Symmetric occluders (68.8%) were more frequently implanted than asymmetric devices (31.2%). Preoperative hemodynamic indices, including RVSP and right atrial volume, were comparable between groups (P > 0.05).

Univariate analysis of echocardiographic predictors

Univariate analysis across three timepoints (preoperative, immediate postoperative, and 1-year follow-up) revealed significant differences in echocardiographic and device-related measurements between the two groups (**Table 2**). Observation group demonstrated consistently larger tricuspid annular diameters than the control group at all timepoints: preoperative (42.1 ± 4.8 mm vs. 38.3 ± 5.1 mm, P < 0.001), immediate postoperative (43.5 ± 5.2 mm vs. 39.1 ± 4.9 mm, P < 0.001), and 1-year follow-up (44.2 ± 5.5 mm vs. 39.5 ± 5.3 mm, P < 0.001). Similarly, coaptation height was significantly lower in the observation group at baseline (6.2 ± 1.5 mm vs. 7.8 ± 1.7 mm, P = 0.003), immediate postoperative (5.8 ± 1.4 mm vs. 7.2 ± 1.6 mm, P < 0.001), and 1-year follow-up (5.5 ± 1.3 mm vs. 7.0 ± 1.5 mm, P < 0.001). Occluder positional deviation was markedly greater in the observation group both immediately after implantation (4.2 ± 1.5 mm vs. 2.1 ± 1.0 mm, P < 0.001) and at 1-year follow-up (3.5 ± 1.2 mm vs. 1.8 ± 0.9 mm, P < 0.001). In contrast, RVSP, right atrial/ventricular volumes, and TAPSE showed no significant

Table 2. Temporal trends in echocardiographic and device-related measurements

Variable	Timepoint	Observation Group (n = 26)	Control Group (n = 83)	Statistical Value	*P*-value
Tricuspid Annular Diameter (mm)	Preoperative	42.1 ± 4.8	38.3 ± 5.1	t = 4.91	< 0.001
	Immediate Postop	43.5 ± 5.2	39.1 ± 4.9	t = 5.34	< 0.001
	1-Year Follow-up	44.2 ± 5.5	39.5 ± 5.3	t = 5.67	< 0.001
	P-value	< 0.001	0.120		
Coaptation Height (mm)	Preoperative	6.2 ± 1.5	7.8 ± 1.7	t = 3.05	0.003
	Immediate Postop	5.8 ± 1.4	7.2 ± 1.8	t = 3.42	< 0.001
	1-Year Follow-up	5.5 ± 1.4	7.0 ± 1.5	t = 3.78	< 0.001
	P-value	0.001	0.061		
TAPSE (mm)	Preoperative	18.4 ± 3.2	19.1 ± 3.5	t = 1.21	0.230
	Immediate Postop	17.9 ± 3.0	18.8 ± 3.4	t = 1.45	0.149
	1-Year Follow-up	17.3 ± 2.9	18.5 ± 3.1	t = 1.89	0.061
	P-value	0.015	0.210		
RVSP (mmHg)	Preoperative	32.4 ± 6.2	31.8 ± 5.9	t = 0.620	0.540
	Immediate Postop	33.1 ± 6.5	32.0 ± 6.1	t = 0.885	0.382
	1-Year Follow-up	33.8 ± 6.7	32.3 ± 6.1	t = 1.234	0.220
	P-value	0.132	0.452		
Right Atrial Volume (mL/m^2)	Preoperative	41.5 ± 8.7	40.2 ± 9.1	t = 0.936	0.354
	Immediate Postop	43.2 ± 9.0	41.0 ± 8.8	t = 1.255	0.213
	1-Year Follow-up	44.8 ± 9.5	41.5 ± 9.3	t = 1.673	0.097
	P-value	0.008	0.180		
Occluder Positional Deviation (mm)	Immediate Postop	4.2 ± 1.5	2.1 ± 1.0	U = 892	< 0.001
	1-Year Follow-up	3.5 ± 1.2	1.8 ± 0.9	U = 1024	< 0.001
	P-value	0.043	0.322		
Asymmetric Occluder, n (%)		9 (34.6%)	15 (18.1%)	χ^2 = 5.432	0.020
Device Size > 30 mm, n (%)		11 (42.3%)	29 (34.9%)	χ^2 = 1.010	0.315
Device Size (mm)		28.5 (24-32)	27.0 (23-31)	U = 3892	0.210
Procedural Time (min)		68.3 ± 18.4	65.7 ± 20.1	t = 0.851	0.400

Notes: TAPSE, tricuspid annular plane systolic excursion; RVSP, right ventricular systolic pressure. Data are presented as mean ± SD or n (%). Statistical tests: Independent t-test (parametric) or Mann-Whitney U test (non-parametric) for continuous variables; chi-square test for categorical variables.

intergroup differences at any timepoint (P > 0.05).

Within-group longitudinal revealed progressive tricuspid annular dilation in the observation group over time (preoperative to 1-year: Δ = +2.1 mm, P < 0.001), whereas the control group remained stable (Δ = +1.2 mm, P = 0.120). Coaptation height declined significantly in the observation group (Δ = -0.7 mm, P = 0.001) but not in controls (Δ = -0.8 mm, P = 0.060). TAPSE showed a gradual reduction in the observation group (preoperative to 1-year: Δ = -1.1 mm, P = 0.015) but remained unchanged in the control group (Δ = -0.6 mm, P = 0.210). Right atrial volume increased significantly in the observation group (Δ = +3.3 mL/m^2, P = 0.008), but with no significant change in control group (Δ = +1.3 mL/m^2, P = 0.180). RVSP changes were nonsignificant in both groups (P = 0.132, P = 0.450). Occluder positional deviation decreased slightly in the observation group from immediate postoperative to 1-year follow-up (Δ = -0.7 mm, P = 0.043), whereas the control group showed no change (Δ = -0.3 mm, P = 0.320) (**Figures 2**, **3**).

Multivariate logistic regression model

Variables with P < 0.1 in univariate analysis, including preoperative tricuspid annular diameter, coaptation height, occluder positional deviation, and asymmetric occluder type, were entered into a multivariate logistic regression

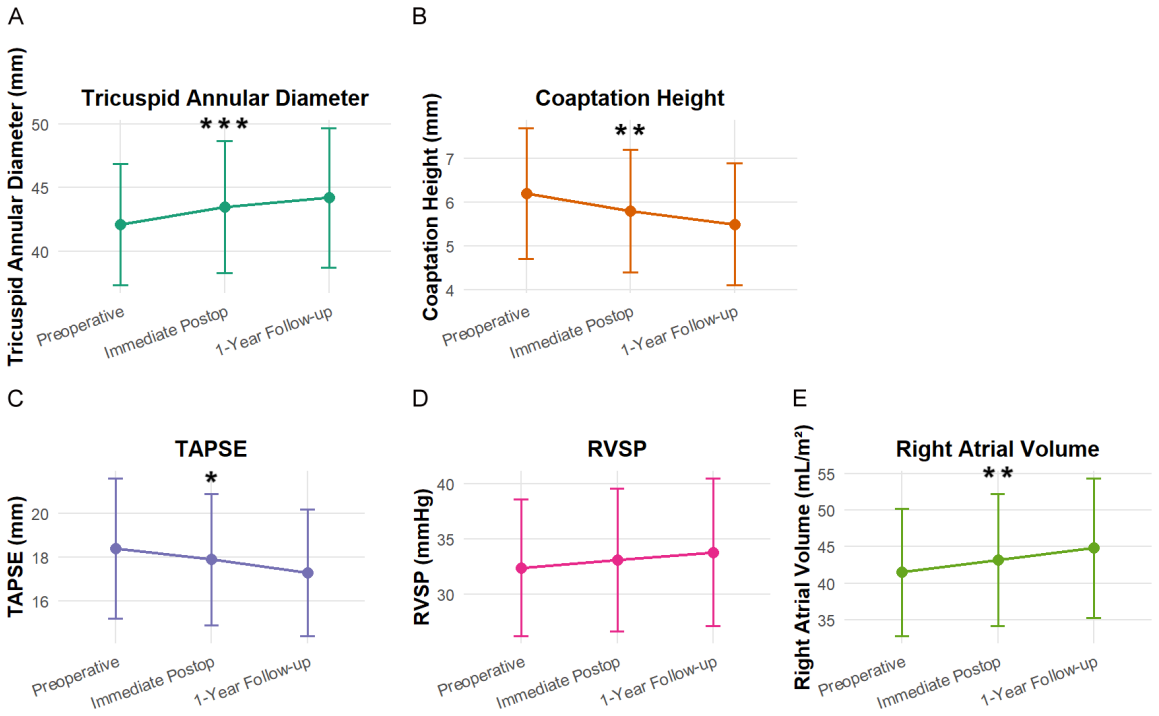

Figure 2. Longitudinal changes in echocardiographic measurements in observation group. A. Tricuspid annular diameter over time; B. Coaptation height over time; C. TAPSE over time; D. RVSP over time; E. Right atrial volume over time. Error bars represent ± 1 SD around the mean at each timepoint (Preoperative, Immediate Postop, 1-Year Follow-up). *P < 0.05, **P < 0.01, ***P < 0.001. TAPSE, tricuspid annular plane systolic excursion; RVSP, right ventricular systolic pressure.

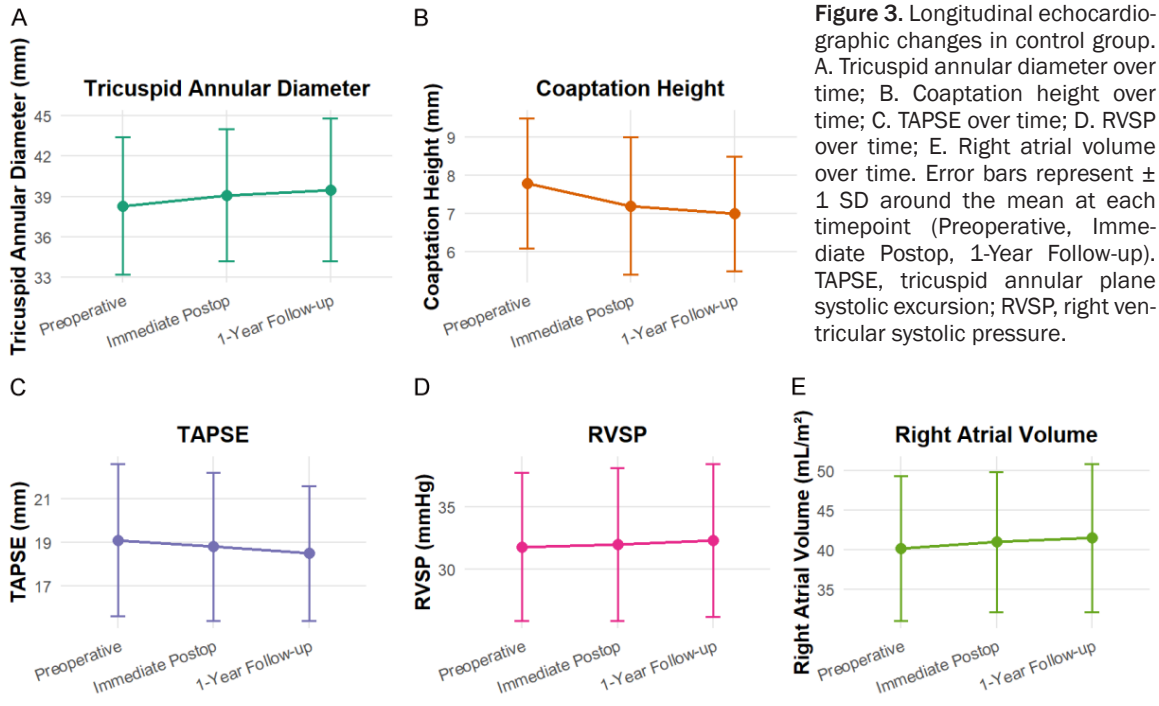

Figure 3. Longitudinal echocardiographic changes in control group. A. Tricuspid annular diameter over time; B. Coaptation height over time; C. TAPSE over time; D. RVSP over time; E. Right atrial volume over time. Error bars represent ± 1 SD around the mean at each timepoint (Preoperative, Immediate Postop, 1-Year Follow-up). TAPSE, tricuspid annular plane systolic excursion; RVSP, right ventricular systolic pressure.

model with backward stepwise elimination (exit criterion P > 0.05). ΔTricuspid Annular Diameter (preoperative to 1-year change) was included as a continuous variable.

Table 3. Variable coding scheme for multivariate logistic regression model

Variable	Type	Coding/Scaling	Reference Category
Δ Tricuspid Annular Diameter	Continuous	Per 1-mm increase	N/A
Occluder Positional Deviation	Continuous	Per 1-mm increase	N/A
Asymmetric Occluder	Categorical	0 = Symmetric, 1 = Asymmetric	Symmetric (0)
Preoperative TR Grade	Categorical	0 = Mild, 1 = Moderate	Mild (0)
Coaptation Height	Continuous	Per 1-mm increase	N/A

Δ Represents the change in tricuspid annular diameter from pre-operative to post-operative measurement.

Table 4. Multivariate Logistic Regression Analysis of Predictors for Postoperative TR Worsening

Variable	β	SE	Wald χ^2	df	Adjusted OR (95% CI)	*P*-value
Δ Tricuspid Annular Diameter (per 1 mm)	0.278	0.082	11.42	1	1.32 (1.12-1.56)	0.001
Occluder Positional Deviation (per 1 mm)	0.880	0.176	25.11	1	2.41 (1.68-3.45)	< 0.001
Asymmetric Occluder (vs. Symmetric)	0.372	0.248	2.25	1	1.45 (0.89-2.36)	0.136
Preoperative TR Grade (Moderate vs. Mild)	0.165	0.252	0.43	1	1.18 (0.72-1.93)	0.512
Coaptation Height (per 1 mm)	-0.083	0.084	0.98	1	0.92 (0.78-1.09)	0.324
Constant	-3.901	0.879	19.69	1	-	< 0.001

Notes: β, regression coefficient; SE, standard error; Wald χ^2, Wald chi-square statistic; df, degrees of freedom; OR, odds ratio; CI, confidence interval; TR, tricuspid regurgitation. Variable definitions: Δ Tricuspid Annular Diameter: Change from preoperative to 1-year follow-up (continuous). Positional Deviation: Immediate postoperative measurement (continuous). Reference categories: TR Grade: Mild; Occluder Type: Symmetric; Model fit: Hosmer-Lemeshow test: $\chi^2 = 6.32$, P = 0.612; Nagelkerke $R^2 = 0.402$.

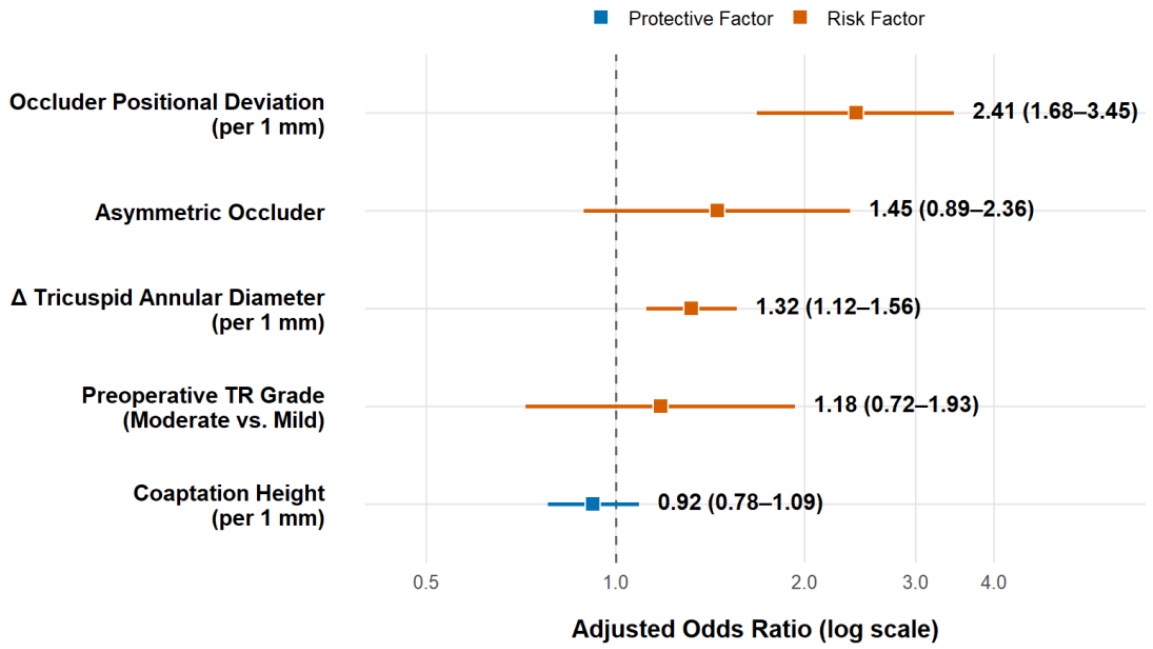

Figure 4. Forest plot for predicting postoperative TR deterioration using multivariate logistic regression. The vertical dashed line at OR = 1 represents no effect; orange markers denote independent risk factors (OR > 1), blue markers denote a protective (OR < 1) effect. TR, tricuspid regurgitation; OR, odds ratio.

The final model identified occluder positional deviation (β = 0.880, SE = 0.176, Wald χ^2 = 25.11, df = 1; OR = 2.41, 95% CI: 1.68-3.45, P < 0.001) and ΔTricuspid Annular Diameter (β = 0.278, SE = 0.082, Wald χ^2 = 11.42, df = 1; OR = 1.32 per 1 mm, 95% CI: 1.12-1.56, P = 0.001) as independent risk factors for postoperative TR worsening. Asymmetric occluder type and baseline TR grade were not statistically significant (**Tables 3**, **4**; **Figure 4**).

Table 5. Predictive performance of individual measurements and combined model

Variable	AUC (95% CI)	Sensitivity (%)	Specificity (%)	Optimal Cutoff
Δ Tricuspid Annular Diameter	0.762 (0.68-0.82)	70.1	74.6	≥ 2.0 mm
Occluder Positional Deviation	0.774 (0.71-0.85)	75.4	79.8	≥ 3.0 mm
Combined Model	0.802 (0.76-0.88)	76.9	81.3	-

Notes: AUC: Area under the ROC curve; CI, confidence interval; higher values indicate better discrimination. Optimal Cutoff: Determined using Youden's index. Combined Model: Derived from multivariate logistic regression coefficients (probability score). Δ Represents the change in tricuspid annular diameter from pre-operative to post-operative measurement.

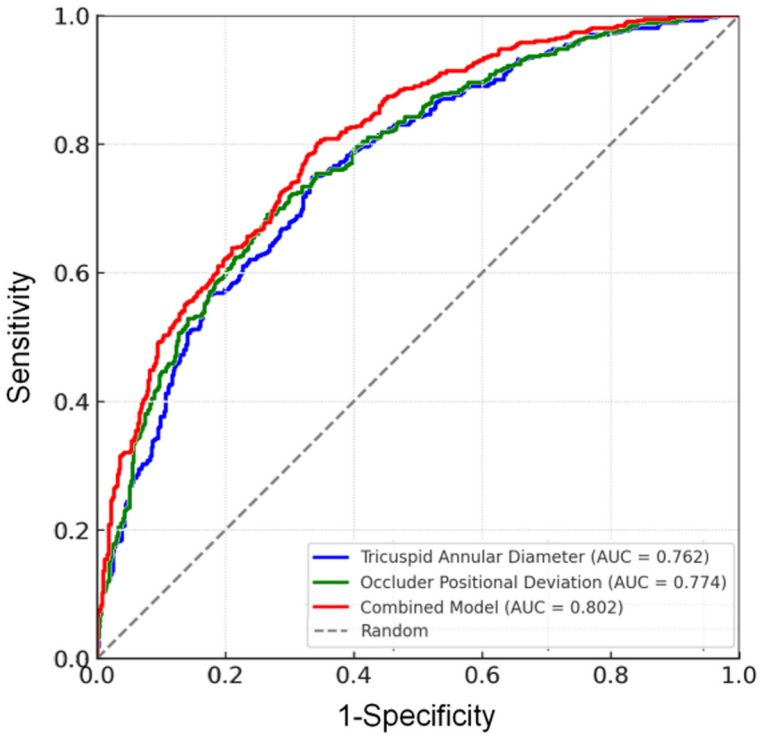

Figure 5. Receiver operating characteristic (ROC) curves for three predictive models. The gray dashed line represents the reference line for random classification (AUC [Area under the ROC curve] = 0.5).

Predictive model performance

The predictive performance of individual measures and the combined model was evaluated using ROC curve analysis, with comparisons conducted using the DeLong test. Δ Tricuspid annular diameter demonstrated an AUC of 0.762 (95% CI: 0.68-0.82), with an optimal discrimination at a cutoff of ≥ 2.0 mm (sensitivity: 70.1%; specificity: 74.6%). Occluder positional deviation showed an AUC of 0.774 (95% CI: 0.71-0.85) with optimal cutoff of ≥ 3.0 mm (sensitivity: 75.4%; specificity: 79.8%). The combined model integrating both these measures exhibited significantly superior discriminative ability (AUC = 0.802, 95% CI: 0.76-0.88; sensitivity of 76.9% and specificity of 81.3% at optimal probability threshold 0.41). Formal DeLong test comparisons confirmed that the combined model outperformed the individual measures (P = 0.016, P = 0.032) (**Table 5**; **Figure 5**).

Subgroup validation

To assess the consistency of the predictive model across occluder types, Bland-Altman analysis was performed in subgroups stratified by device symmetry (symmetric vs. asymmetric occluders). In the symmetric occluder subgroup (n = 150), the mean bias between predicted and observed TR worsening probabilities was -0.03 (95% limits of agreement: -0.18 to 0.12), indicating no systematic prediction bias. In the asymmetric occluder subgroup (n = 68), the mean bias was -0.05 (95% limits: -0.21 to 0.11), demonstrating comparable agreement. Both subgroups showed homoscedastic variance (P > 0.05 via Levene's test), confirming stable model performance regardless of device design (**Table 6**; **Figure 6**). Interaction analysis further confirmed that the effects of Δ annular diameter and occluder positional deviation on TR progression were independent of device symmetry (all P > 0.05, **Table 7**; **Figure 7**).

Discussion

This study demonstrates that postoperative TR worsening following transcatheter closure of ASD with PFO using domestic occluders is predominantly driven by mechanical stress-induced remodeling of the tricuspid annulus

Table 6. Bland-Altman analysis by occluder subgroup

Subgroup	Mean Bias	SD of Bias	95% Limits of Agreement	*P*-value for Heteroscedasticity
Symmetric Occluder	-0.03	0.08	-0.18 to 0.12	0.452
Asymmetric Occluder	-0.05	0.09	-0.21 to 0.11	0.387

Note: SD, standard deviation; 95% Limits of Agreement = mean bias ± 1.96×SD; Symmetric Occluder, symmetric cardiac occluder device; Asymmetric Occluder, asymmetric cardiac occluder device; Heteroscedasticity refers to non-constant variance of measurement differences across the range of values.

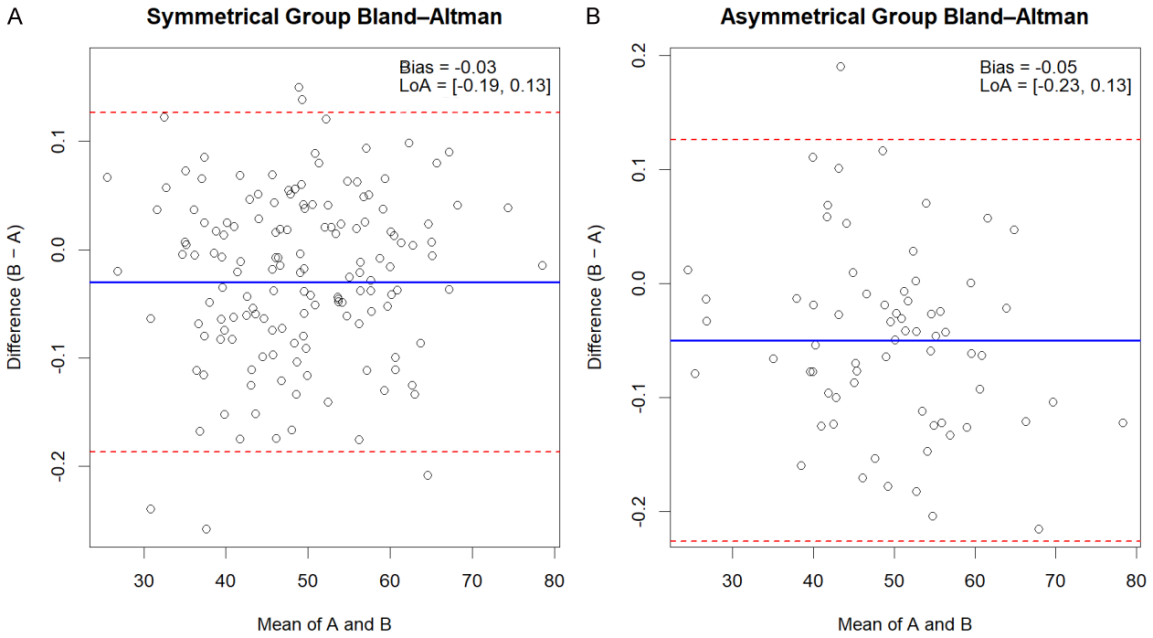

Figure 6. Bland-Altman analysis of predicted and observed TR worsening probabilities by occluder symmetry. A. Bland-Altman plot for the symmetrical occluder subgroup (n = 75): blue solid line = mean bias (-0.03); red dashed lines = 95% limits of agreement (-0.18 to 0.12). B. Bland-Altman plot for the asymmetrical occluder subgroup (n = 34): blue solid line = mean bias (-0.05); red dashed lines = 95% limits of agreement (-0.21 to 0.11).

Table 7. Interaction analysis for occluder types

Interaction Term	Adjusted OR	95% CI	*P*-value
Δ Annular Diameter × Asymmetric	1.12	0.93-1.35	0.214
Positional Deviation × Asymmetric	0.87	0.64-1.19	0.376

Note: OR, odds ratio; CI, confidence interval; Δ Annular Diameter, change in tricuspid annular diameter; Positional Deviation, degree of device malposition; Asymmetric, asymmetric cardiac occluder device (reference: symmetric occluder). Interaction terms evaluate effect modification between occluder type and morphologic data.

and device malposition. Multivariate analysis identified Δ tricuspid annular diameter (OR = 1.32 per 1 mm increase) and occluder positional deviation (OR = 2.41 per 1 mm deviation) as independent predictors, with the combined model achieving an AUC of 0.802, surpassing previous models that relied on static anatomical or hemodynamic parameters [12]. These findings align with biomechanical studies showing that device-induced septal stiffening redistributes RV systolic forces, generating asymmetric traction on the tricuspid annulus [13]. Over time, this mechanical stress triggers extracellular matrix degradation and annular dilation - a process exacerbated by chronic RV volume overload, as evidenced by progressive right atrial expansion (P = 0.008) in the TR-worsening group [14]. The observed 2.41-fold risk increase per millimeter of positional deviation underscores the critical role of device geometry in modulating annular strain. Finite element analyses have shown that even minor deviations alter leaflet coaptation forces, creating localized stress concentrations that accelerate valvular dysfunction [15].

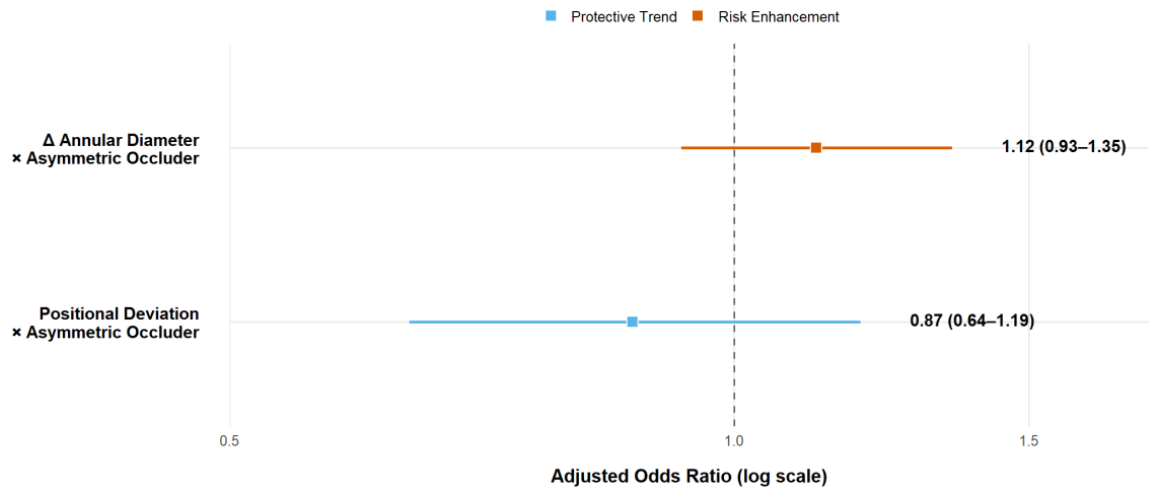

Figure 7. Forest plot for interactive analysis of occluder types.

This interaction between structural remodeling and procedural factors explains the superior predictive accuracy of the combined model compared to isolated measurements.

The clinical implications of these findings are profound. Intraprocedural echocardiographic monitoring of annular dimensions and device alignment could mitigate the risk of TR progression, particularly in patients with baseline annular diameters exceeding 40 mm - a threshold associated with a 3.5-fold higher risk of postoperative deterioration in our cohort. Real-time annular measurement, combined with fluoroscopic guidance to minimize positional deviation, may reduce the need for reinterventions, as malposition correction during implantation has been shown to lower TR progression rates in mitral valve interventions [16]. Furthermore, the model's consistency across occluder subtypes (symmetric vs. asymmetric) challenges earlier reports linking device asymmetry to adverse outcomes [17], suggesting that modern domestic occluders may incorporate design refinements such as enhanced flexibility or reduced radial force, that mitigate mechanical interactions with the tricuspid apparatus [18]. This finding is particularly relevant in regions where domestic devices are widely adopted due to cost constraints, as it supports their safety profile while highlighting the need for standardized implantation protocols.

The dynamic nature of annular remodeling captured in this study represents a shift in post-procedural surveillance. Traditional follow-up protocols emphasizing hemodynamic metrics like RVSP may overlook early structural changes, as RVSP remained stable in both groups despite significant annular dilation. Instead, serial echocardiographic assessment of annular dimensions and coaptation height - measures that exhibited progressive deterioration in the TR-worsening group - may facilitate earlier intervention. For instance, a Δ annular diameter ≥ 2 mm at 1-year follow-up might prompt consideration of prophylactic annuloplasty, a strategy shown to reduce TR recurrence in high-risk surgical patients [19]. Additionally, the low incidence of adverse events (e.g., 7.7% arrhythmias, 1.9% device embolization) reaffirms the safety of domestic occluders, aligning with recent multicenter registries reporting comparable complication profiles to international devices [20]. However, the absence of severe pulmonary hypertension in our cohort limits generalizability to advanced disease states, where annular dynamics may be influenced by elevated RV afterload [21].

Despite these advancements, limitations inherent to retrospective single-center designs necessitate cautious interpretation. Unmeasured confounders, such as genetic predisposition to annular dilation or subclinical myocardial fibrosis, may partially explain the observed associations [22]. Additionally, while adherence to ASE guidelines minimized measurement variability, inter-observer differences in annular diameter quantification persist across echocardiographic laboratories [11], underscoring the need for automated quantification tools.

Moreover, the 1-year follow-up period, though sufficient to capture early remodeling, precludes assessment of late TR progression, which may occur years post-implantation due to cumulative mechanical stress [5]. Future prospective studies should integrate advanced imaging modalities like 3D echocardiography or cardiac MRI to quantify annular strain patterns and validate the model in diverse populations, including those with congenital tricuspid anomalies or prior cardiac surgeries.

Conclusion

Risk stratification for TR after ASD/PFO closure was redefined by prioritizing dynamic structural metrics over conventional static measurements. The validated model not only enhances preoperative risk counseling but also provides a framework for intraprocedural decision-making, emphasizing the importance of annular preservation and precise device positioning. As transcatheter therapies continue to evolve, these insights will help to update surveillance protocols that prioritize longitudinal anatomical assessment, ultimately improving long-term outcomes in this growing patient population.

Acknowledgements

This study was supported by the Medical Science Research Project Plan Project of Hebei Provincial Health and Health Commission (No. 20231024).

Informed consent was obtained from all the participants.

Disclosure of conflict of interest

None.

Address correspondence to: Ning Zhang, Department of Ultrasound, The First Hospital of Hebei Medical University, No. 89 Donggang Road, Yuhua District, Shijiazhuang 050000, Hebei, China. E-mail: m13803396138@163.com

References

[1] Kheiwa A, Hari P, Madabhushi P and Varadarajan P. Patent foramen ovale and atrial septal defect. Echocardiography 2020; 37: 2172-2184.

[2] Xu Q, Fa H, Yang P, Wang Q and Xing Q. Progress of biodegradable polymer application in cardiac occluders. J Biomed Mater Res B Appl Biomater 2024; 112: e35351.

[3] Nappi F. Assessing emerging causes of mitral regurgitation: atrial functional mitral regurgitation. J Int Med Res 2024; 52: 3000605241240583.

[4] Fortuni F, Dietz MF, Butcher SC, Prihadi EA, van der Bijl P, Ajmone Marsan N, Delgado V and Bax JJ. Prognostic implications of increased right ventricular wall tension in secondary tricuspid regurgitation. Am J Cardiol 2020; 136: 131-139.

[5] Omori T, Uno G, Shimada S, Rader F, Siegel RJ and Shiota T. Impact of new grading system and new hemodynamic classification on long-term outcome in patients with severe tricuspid regurgitation. Circ Cardiovasc Imaging 2021; 14: e011805.

[6] Mathur M, Meador WD, Jazwiec T, Malinowski M, Timek TA and Rausch MK. Tricuspid valve annuloplasty alters leaflet mechanics. Ann Biomed Eng 2020; 48: 2911-2923.

[7] Volpato V, Mor-Avi V, Veronesi F, Addetia K, Yamat M, Weinert L, Genovese D, Tamborini G, Pepi M and Lang RM. Three-dimensional echocardiography investigation of the mechanisms of tricuspid annular dilatation. Int J Cardiovasc Imaging 2020; 36: 33-43.

[8] Nyrnes SA, Løvstakken L, Døhlen G, Skogvoll E, Torp H, Skjaerpe T, Norgård G, Samstad S, Graven T and Haugen BO. Blood flow imaging in transesophageal echocardiography during atrial septal defect closure: a comparison with the current references. Echocardiography 2015; 32: 34-41.

[9] Bach Y, Abrahamyan L, Lee DS, Dharma C, Day J, Parker JD, Benson L, Osten M and Horlick E. Long-term outcomes of adults with tricuspid regurgitation following transcatheter atrial septal defect closure. Can J Cardiol 2022; 38: 330-337.

[10] Nassif M, van der Kley F, Abdelghani M, Kalkman DN, de Bruin-Bon RHACM, Bouma BJ, Schalij MJ, Koolbergen DR, Tijssen JGP, Mulder BJM and de Winter RJ. Predictors of residual tricuspid regurgitation after percutaneous closure of atrial septal defect. Eur Heart J Cardiovasc Imaging 2019; 20: 225-232.

[11] Lang RM, Badano LP, Mor-Avi V, Afilalo J, Armstrong A, Ernande L, Flachskampf FA, Foster E, Goldstein SA, Kuznetsova T, Lancellotti P, Muraru D, Picard MH, Rietzschel ER, Rudski L, Spencer KT, Tsang W and Voigt JU. Recommendations for cardiac chamber quantification by echocardiography in adults: an update from the American Society of Echocardiography and the European Association of Cardiovascular

Imaging. J Am Soc Echocardiogr 2015; 28: 1-39, e14.
[12] Shamekhi J, Sugiura A, Tabata N, Al-Kassou B, Weber M, Sedaghat A, Werner N, Grube E, Nickenig G and Sinning JM. Impact of tricuspid regurgitation in patients undergoing transcatheter aortic valve replacement. JACC Cardiovasc Interv 2020; 13: 1135-1137.
[13] Jonnagiri R, Sundström E, Gutmark E, Anderson S, Pednekar AS, Taylor MD, Tretter JT and Gutmark-Little I. Influence of aortic valve morphology on vortical structures and wall shear stress. Med Biol Eng Comput 2023; 61: 1489-1506.
[14] Chango-Azanza DX, Munin M, Sanchez G, Raggio I, Pelayo ME, Garro H, Arevalo M, Carbajales J, Makhoul S and Ronderos R. Insights of tricuspid regurgitation mechanisms in patients with right ventricular apical pacing by three-dimensional echocardiography. Echocardiography 2023; 40: 903-915.
[15] Kong F, Pham T, Martin C, McKay R, Primiano C, Hashim S, Kodali S and Sun W. Finite element analysis of tricuspid valve deformation from multi-slice computed tomography images. Ann Biomed Eng 2018; 46: 1112-1127.
[16] Carpenito M, De Luca VM, Cammalleri V, Piscione M, Antonelli G, Gaudio D, Strumia A, Di Pumpo AL, Mega S, Carassiti M, Grigioni F and Ussia GP. Edge-to-edge repair for tricuspid regurgitation: 1-year follow-up and clinical implications from the TR-Interventional Study. J Cardiovasc Med (Hagerstown) 2025; 26: 50-57.
[17] Chen W, Li T, Lei X and Liu H. An observational study of symmetrical VSD occluder for transcatheter closure of ruptured sinus of Valsalva aneurysm. Exp Ther Med 2024; 27: 244.
[18] Zhang Z and Ding J. Successful occluder removal and reocclusion of an atrial septal defect after occluder immigration to aortic arch: a case report. J Cardiothorac Surg 2024; 19: 575.
[19] Fortuni F, Dietz MF, Prihadi EA, van der Bijl P, De Ferrari GM, Bax JJ, Delgado V and Marsan NA. Ratio between vena contracta width and tricuspid annular diameter: prognostic value in secondary tricuspid regurgitation. J Am Soc Echocardiogr 2021; 34: 944-954.
[20] Weckbach LT, Stolz L, Doldi PM, Glaser H, Ennin C, Kothieringer M, Stocker TJ, Näbauer M, Kassar M, Bombace S, Kresoja KP, Lurz P, Praz F, Thiele H, Rudolph V, Massberg S and Hausleiter J. Relevance of residual tricuspid regurgitation for right ventricular reverse remodelling after tricuspid valve intervention in patients with severe tricuspid regurgitation and right-sided heart failure. Eur J Heart Fail 2024; [Epub ahead of print].
[21] Zack CJ, Fender EA, Chandrashekar P, Reddy YNV, Bennett CE, Stulak JM, Miller VM and Nishimura RA. National trends and outcomes in isolated tricuspid valve surgery. J Am Coll Cardiol 2017; 70: 2953-2960.
[22] Prihadi EA, Delgado V, Leon MB, Enriquez-Sarano M, Topilsky Y and Bax JJ. Morphologic types of tricuspid regurgitation: characteristics and prognostic implications. JACC Cardiovasc Imaging 2019; 12: 491-499.